Received: 22 August 2022 | Revised: 02 November 2022 | Accepted: 17 November 2022

DOI: 10.5185/amlett.2023.021720

OPEN ACCESS

RESEARCH

Synthesis, Characterization and Studies of Nanosized $BaSnO_3$ and Its Poly (vinylalcohol) Nanocomposite Film

Arunkumar Lagashetty[1,*] | Jayasurya H[1] | Swati[1] | Netravati[1] | Leelanagalaxmi[1] | Chitralekha Alur[2] | Sangappa K Ganiger[3]

[1]Department of Studies in Chemistry, Vijayanagara Sri Krishnadevaraya University, Ballari 583105, Karnataka, India
[2]Department of Physics, Sharanabasaveshwar College of Science, Kalaburagi 585103, Karnataka, India
[3]Department of Physics, Government Engineering College Raichur - 584135, Karnataka, India

***Corresponding author:**
Arunkumar Lagashetty
E-mail: arun.lagashetty@gmail.com

ABSTRACT

Synthesis of nanosized materials integrates the materials synthetic technology. Nanosized bimetallic oxides constitute class materials in concerned with its applications. The present work reports the synthesis of barium stannate ($BaSnO_3$)nanopowder by self-propagating combustion reaction using polyvinyl alcohol (PVA) as a fuel. Initially basic oxides barium oxide (BaO) and tin oxide (SnO_2) are also prepared by combustion route. Further barium stannate-PVA nanocomposite ($BaSnO_3$-PVA) is prepared by dispersion of $BaSnO_3$ material into PVA matrix using solvent casting method. Structural characterization of oxide and nanocomposite was studied by X-ray diffraction (XRD) tool and bonding nature by Fourier transfer infrared study (FT-IR) respectively. Thermal behavior of both the sample is well studied by thermo gravimetric analysis (TGA). Electrochemical study of the sample is carried out by cyclic voltammetry (CV) instrumentation. Varied morphology and particle size of the sample was analysed through Transmission electron microscope (TEM) tool.

KEYWORDS

Nanocomposite, $BaSnO_3$, PVA, TEM, TGA, CV.

INTRODUCTION

Metal stannates are important in material systems due to their excellent physical properties and chemical properties [**1**]. These perovskite-type oxides show flexible structure and are easy for ionic doping and oxygen non-stoichiometry. This kind of structural arrangement can form a vast set of technologically important materials for various applications [**2-3**]. $BaSnO_3$ is one of the stannate material substituted with barium forms a cubic perovskite-type oxide material that behaves as n-type semiconductor and remains stable at high temperatures. This material shows various applications such as thermally stable capacitors, humidity sensors, gas sensors, etc. [**4-5**]. It also finds applications in optical processing [**6**], in capacitors, in ceramic boundary layers [**7**] and as a promising material to produce gas phase sensors for the detection of carbon monoxide and carbon dioxide [**8-9**]. It is reported in the literature that, La doped $BaSnO_3$ exhibits high electrical mobility at room temperature and superior thermal stability at high temperatures [**10**]. Various techniques have been employed to synthesize $BaSnO_3$nanomaterial out of which solid state combustion method finds much importance because of its simplicity and high yield. Barium stannate has been studied for its interesting electronic property due to wide band gap pervoskite oxide finds many applications [**11-16**]. High mobility of this material consumes low power and hence finds applications in power electronics. [**17-18**]. Barium stanate bimetallic oxide material composed with Ba and Sn metals. This material is classified under n-type semiconductor materials and is stable for high temperature [**19**]. It is one of the reinforcement materials especially in preparation of polymer composites in which polymer is considered as matrix materials. Various compositions of these two materials lead new class of composite materials for multiple applications. Nanosized

$BaSnO_3$ material has lot of commercial demand due to its transport properties [**20**]. In addition, it is studied widely due to its potential applications in the field of sensors, photocatalyst and capacitors [**21**].

A composite material consists of two or more materials, out of which one is reinforcement and others are matrix materials. The composite may contain metals, ceramics, and other polymers as a matrix and as reinforcement. In polymer composite, polymeric materials have been used as the matrix material and other is a reinforcement material. A polymer material with a reinforcement of ceramic materials penetrates throughout the structural polymer leads to a new class of materials with new design and new properties. Combination of different materials with differing in compositions, in which, the individual constituents retain their separate identities even after mixing. These separate constituents act together to give the necessary mechanical strength or stiffness to the composite part. Composite material is a material composed of two or more distinct phases (matrix phase and dispersed phase) and having bulk properties significantly different from those of any of the constituents. Matrix phase is the primary phase having a continuous character. Matrix is usually more ductile and less hard phase. It holds the dispersed phase and shares a load with it. Dispersed (reinforcing) phase is embedded in the matrix in a discontinuous form. This secondary phase is called the dispersed phase. Dispersed phase is usually stronger than the matrix, therefore, it is sometimes called reinforcing phase. [**22-23**]. Present work is reporting that, the synthesis of $BaSnO_3$ materials by solid state combustion method using polymer as an efficient fuel. Reactants undergo self-Propagating combustion reaction with polymer fuel to form the desired product. $BaSnO_3$-PVA nanocomposite was prepared to study its properties.

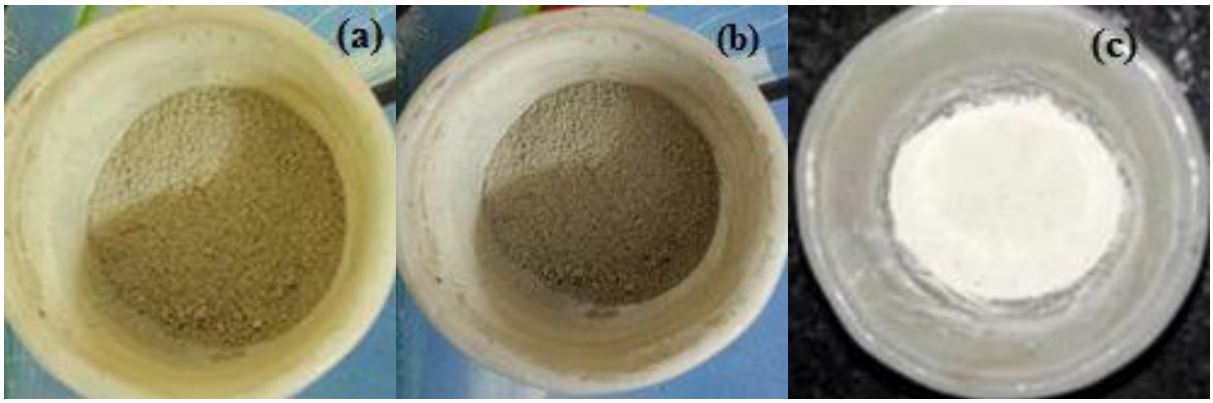

Fig. 1. Optical image of combustion derived (a) BaO sample (b) SnO_2 sample(c) $BaSnO_3$ sample.

EXPERIMENTAL

Materials and methods

Chemicals used in the present experimentation are of AR grade and are perchaged from Merck (Mumbai, India). Double distilled water is used as a solvent and chromic acid rinsed glass wares are used in the experimentation. Self-propagating combustion method is used for the synthesis of barium stannate nanomaterial and solvent casting method is used for the synthesis of PVA nanocomposite.

Synthesis of BaO and SnO_2 nanomaterials

Barium chloride ($BaCl_2$) wasmixed with PVA in the weight ratio 1:5 and grounded well in a pestle and mortar which forms a combustion able reaction mixture. The resultant solid mixture was transferred into china dish and heated in open air atmosphereuntil the carbonaceous gases was completely evolved. Then, it is transferred into silica crucible and ignited at around 1000°C in a muffle furnace. During the combustion process, it was observed that, initially PVA melted, then frothed and finally ignited to give BaO as a residue. On cooling to room temperature followed by acetone washing gives yellowish white coloured BaO product and is shown in **Fig. 1(a)**. This reaction occurs with the evolution of large volume of gases and ignites with self-propagation combustion reaction. Similar procedure was adopted in the synthesis of SnO_2, a grayish white SnO_2 as residue was obtained after final combustion process and is as shown in **Fig. 1(b)**[**24**].

Synthesis of $BaSnO_3$

Barium stannate was synthesized by weighing BaO, SnO_2 and PVA in the ratio 1:1:5 and grounded well in a pestle and mortar to form a reaction mixture. The resultant solid was transferred into china dish and pre heated in open air atmosphere. Continue the burning process until the complete evolution of carbonaceous product. The resultant product was grinded well and was transferred into silica crucible for further reaction. Ignite the reaction mixture for about 1400°C in muffle furnace for about 30 minutes. During the reaction, it was observed that, initially PVA melted, frothed and finally forms$BaSnO_2$ as a final product,

which is shown in **Fig. 1(c)**[**25**]. Impurities if any are washed with acetone and dried for desired product. The possible reaction of the combustion process is given below, and its synthetic scheme is given in **Scheme 1**.

$$BaO + SnO \rightarrow BaSnO_3$$

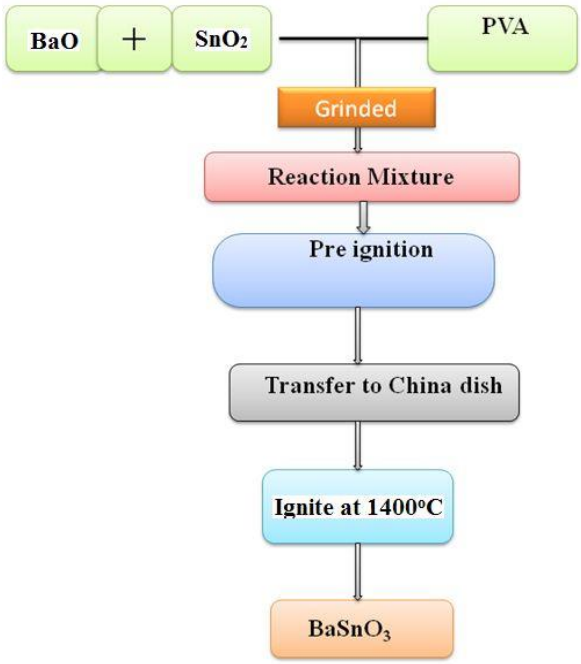

Scheme 1. Synthesis of barium stannate nanoparticles.

Preparation of $BaSnO_3$- PVA composite

Weigh accurately 2g of PVA polymer and dissolved in 5ml of distilled water by continuous stirring to form emulsion of PVA polymer. Add 0.5g as prepared $BaSnO_3$ nanomaterial in to PVA emulsion and stir well for uniform mixing. The solution was poured into petridish uniformly and covers the same with cage cover. Evaporate the solvent under low temperature to form $BaSnO_3$ dispersed thin composite film and is shown in **Fig. 2** [**26**].

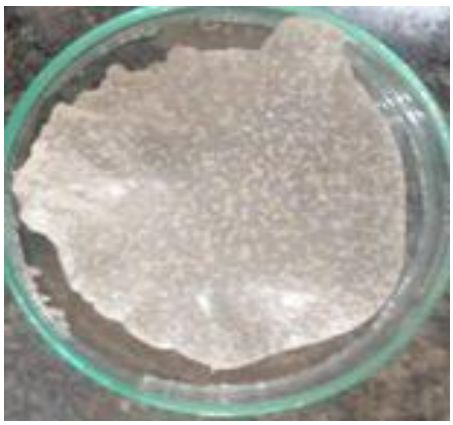

Fig.2. Optical image of $BaSnO_3$- PVA composite.

Characterisation

XRD was employed to study the prepared $BaSnO_3$, and$BaSnO_3$- PVA composite structure with CuKα as radiation source by X' Pert Pro X-ray diffractometer. The bonding natures of the samples are studied using Perkin–Elmer 1600 spectrophotometer in KBr medium. Morphology and particle size of the sample was studied by GEOL GEM1010 transmission electron microscope was acquired at 70kv is used for TEM scanning.

RESULTS AND DISCUSSIONS

FT-IR study

In order to ascertain the molecular nature of the synthesized material, the FT-IR spectrum of the barium stannate sample was scanned and is shown in the **Fig. 3(a)**. In the FT-IR spectra of the sample shows a wide band of –OH group observed at around 3300 cm^{-1}. It is observed from the figure that, the vibrational bands are reflecting below 1000 cm^{-1} are due to metal-oxygen (M-O) bond and peak at 400 cm^{-1} shows the presence of metal-metal (Ba-Sn) vibrational mode. The bond at 2071.54 cm^{-1} is due to stretching vibrational modes. Peak at 1626.02cm^{-1} may be due to carbonyl group and band at 3447.13cm^{-1} corresponding to OH bonding. On the other hand, the observation of FT-IR of its PVA composite (**Fig. 3(b)**) the spectrum reveals that the similar observation with shift in the frequency and addition of additional vibrations clearly shows the formation of $BaSnO_3$- PVA composite. The width of this band is particle size dependent. Therefore, the width of the band is broad for the calcined sample.

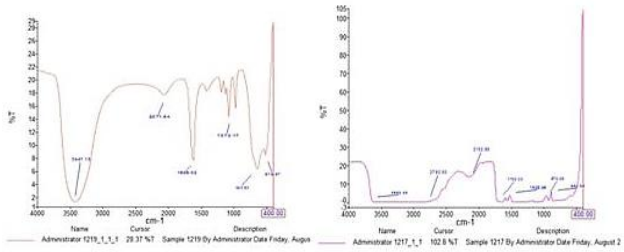

Fig. 3. (a) FT-IR Spectra of $BaSnO_3$ nanomaterials; (b) FT-IR Spectra of $BaSnO_3$- PVA nanocomposite.

TGA study

Fig. 4(a) shows TGA trace of prepared barium stannate nanomaterial. The trace shows the multi step weight loss at different temperature. Initially up to 260°C it indicates the presence of fast degradation due to less percent of moisture content of the sample and second weight loss from 260°C to 500°C indicates the complete degradation of sample. The slow step decomposition followed leads the ash of the sample. **Fig. 4(b)** shows TGA trace of prepared $BaSnO_3$-PVA nanocomposite film. This trace also shows multi step weight loss at different temperature. First step weight loss up to 600°C indicates the removal of moisture content of

the sample and second weight loss from 600°C to 630°C indicates the polymer degradation. It breaks the interaction between the metal oxides with polyvinyl alcohol. The slow step decomposition followed leads to the formation of ash of the sample. TGA trace of $BaSnO_3$-PVA nanocompositeis compared with TGA trace of plain barium stannate shows that the increase in thermal stability of the composite film.

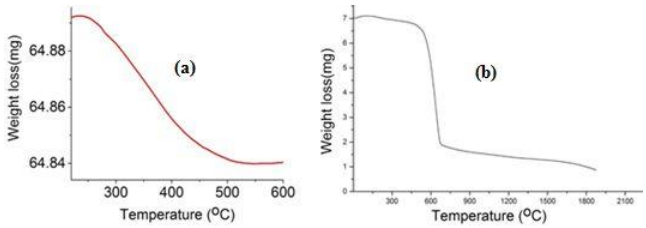

Fig. 4.TGA trace of (a): $BaSnO_3$(b) $BaSnO_3$-PVA nanocomposite.

XRD study

Fig. 5(a) shows the XRD pattern of as prepared $BaSnO_3$nanomaterials. The pattern shows the presence of highly intensed Bragg's reflections indicates the crystalline nature of the sample. The comparison of d-spacing values of the prepared $BaSnO_3$ sample and that of standard JCPDS file with indexed (hkl) values are given in the **Table1**. It is observed from the table that, most of the d-spacing value of the sample matches well with literature data of the $BaSnO_3$ (JCPDS card No. 15-0780) confirms the formation of the $BaSnO_3$ materials. Purity of the sample analyzed in the pattern by the absence of the other reflection. **Fig. 5(b)** shows indexed XRD pattern of $BaSnO_3$-PVA nanocomposite. The pattern shows the presence of some $BaSnO_3$ peaks which are identified in the PVA composite pattern confirms the formation of the composite film. Some peaks of $BaSnO_3$ materials in polymer are masked in the polymer matrix and some reflections shows slight shifting due to matrix complexation.

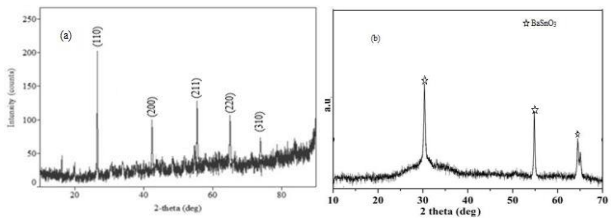

Fig. 5. XRD pattern of (a) $BaSnO_3$ nanomaterial (b) $BaSnO_3$-PVA nanocomposite.

Table 1. Comparison of observed data with literature data of $BaSnO_3$

Sl.No	Observed d-spacing values	Literature d-spacing values	(hkl)
1	2.91	2.9109	(110)
2	2.06	2.0585	(200)
3	1.68	1.6789	(211)
4	1.45	1.4554	(220)
5	1.30	1.2999	(310)

Cyclic Voltametry (CV) Study

Fig. 6 shows CV spectra of as prepared $BaSnO_3$-PVA nanocomposite. It shows the highly intense peak at 0.3V of potential indicates that sensing of mercury by compound. The obtained data indicates that, the prepared compound is good catalyst and good sense of mercury. The GCE/ $BaSnO_3$ nanocomposite was evaluated for the detection of highly toxic Hg (II) by cyclic voltammetry in 0.1 M PBS (pH = 7) (PBS = phosphate buffer solution). 50 microliter Hg(II) solution was added into PBS, a peak appeared at 0.26V on the GCE/$BaSnO_3$ nanocomposite which is responsible for the detection of Hg(II) but the bare GCE did not show an appreciable peak for the addition of analyte. The cyclic voltammetry related to the electro catalytic current for Hg detection at GCE/$BaSnO_3$ was much larger with lesser over potential compared to GCE. So, one can easily find that enhanced peak current and decrease in the over potential established the barium stannate nanocomposite acts as an effective catalyst to activate the reaction for the detection of the analyte.

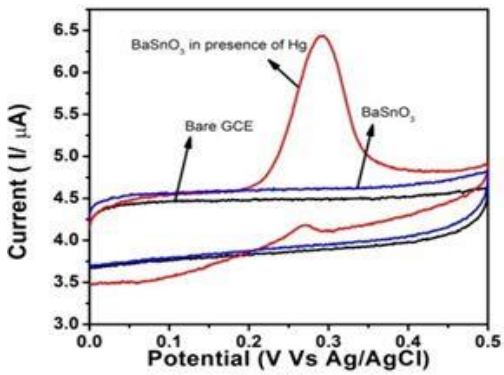

Fig. 6. CV trace of $BaSnO_3$-PVA nanocomposite.

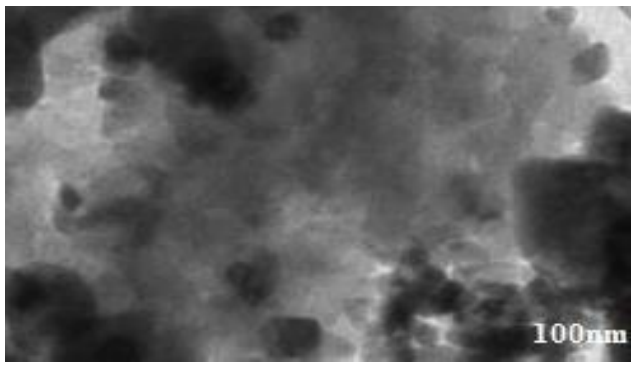

Fig. 7. TEM image of $BaSnO_3$-PVA nanocomposite.

TEM Study

The morphology study and its particle size of the as prepared $BaSnO_3$-PVA nanocomposite sample was studied by transmission electron microscope image and is given in **Fig. 7**. The image shows semi crystalline morphology and spherical particle shape particles fall within the nano range.

The particles seem to be closely joined together to form fine spheres with compactness behavior of some particles. In addition, it is showing irregular arrangement of some particles with high surface area morphology leads to applicable morphology.

CONCLUSIONS

A bimetallic oxide like $BaSnO_3$ is successfully synthesized by self-propagating combustion route. The use of PVA as a fuel in the synthesis combustion derivation and this method may be applied for the synthesis of other bimetallic oxide materials in large scale. The results obtained from the XRD pattern confirm the development of crystallinity in the noncrystalline polymer matrix. The FT-IR spectrum reveals that there is a peak below 1000cm^{-1} which has been associated with the vibration of M-O and M-M bonds in the system. TGA results indicating high thermal stability in the composite materials is due to the addition of crystalline materials in polymer matrix. Cyclic voltametric study revealed that the $BaSnO_3$-PVAnanocomposite acts as an effective catalyst to activate the reaction for the detection of the analyte. Overall, the present attempt demonstrates the composite formation by state-of-the-art technique and careful characterization of $BaSnO_3$ as well as its PVA composite. Cyclic voltametry studies concluding that, the polymer-based barium stannate nanocomposite acts as an effective catalyst to activate the reaction for the detection of the analyte. Further, it may be applicable for varied pervoskite nanocomposite with varied polymers.

ACKNOWLEDGEMENT

The Authors convey their heartfelt thanks to DST-FIST (SR/FST/CSI-003/2016) for the grant provided to procure the required instruments and infrastructure at the chemistry Department of Vijayanagar Sri Krishnadevaraya University Ballari. Our thanks are also due to Prof. A. Venkataraman, the Department of chemistry, Gulbarga University, Kalaburagi for his consistent encouragement and support.

REFERENCES

1. Anh, D.T.; Than,N.T.; *Uni. J. Phy. Appln.*,**2017**, *11(6)*, 235.
2. Gahlawat, S.; Ahmet, I.Y.; Schnell, P.; Levine, I.; Zhang, S.; Ingole, P.P.; Abdi, F.T.; *Chem. Mater.*, **2022**, *22*, 4320.
3. Marikutsa, A.; Rumyantseva, M.; Baranchikov, A.; Gaskov, A.; *Materials.*, **2015**, *8*, 6437.
4. Jinolong, M.; Li, W.; Luo, X.; *Phy. Rev. B*, **2022**, *106*, 045201.
5. Lim, C. Y.; Hee, K.S.; *J. Nanosci. and Nanotech.*,**2020**, *20(9)*, 5498.
6. Zhang, Z.; Xie, E.; *J. Mater. Chem. A*, **2022** (In press)
7. Bradha, M.; Vijayaraghavan, T.; Ashok, A.; *Mater. Lett.*, **2014**, *125*, 187.
8. Galazka, Z.; Transporent Semiconducting oxides, Jenny Stanford Pub, **2020.**
9. Upadyay, S.; Bull. *Mater. Sci.*, **2013**, *36(6)*,1019.
10. John, J.; Pillai, V.P.M.; Thomas, A.R.; Philip, R.; Joseph, J.; Muthunatesan, S.; Ragavendran, V.; Prabhu, R.; IOP Conf. Series: Materials Science and Engineering, **2017**,*195*, 012007
11. Arya, B.B.; Choudhary, R.N.P.; *Cer. Int.* **2022**, *46(4)*, 4222.
12. Sohrab, I.B.; Frederick, J. W.; Cheong, S.W.; Karin, M. R.; Charles, H. A.; *APL Materails.* **2015**, 3, 062510.
13. Xing, S.M.; Shan, C.; Jiang, K.; Zhu, J.J.; Li, Y.W.; Hu, Z.G.; Chu, J.H.; *J. Appl. Phys.*, **2015**, 117, 103107.
14. Woong-Jhae, L,; Hyung, J. K.; Jeonghun, K.; Dong, H. J.; Tai, H. K.; Jeong, H. L.; Kee, H. K.; Annual Review of Material Research, **2017**, 47, 391.
15. Gogova, D.; Suwardi, A.; Kutznetsova, Y.A.; Zat-sepin, A.F.; Mochalov, L.A.; Nezhdanov, A.; Szyszka, B.; *I.J. Adv. Appl. Phy. Res.*, **2017**, 4, 1.
16. Yajun, Z.; Sahoo, M. P. K.; Jie, W.; *Phys. Chem. Phys.*, **2017**,19, 7032.
17. Luo, X.; Oh, Y.S.; Sirenko, A.; Gao,P.; Tyson, T.A.; Char, K.; Cheong, S.W.; *Appl. Phys. Lett.* **2012**,100, 172112.
18. Abhinav, P.; Peng, X.; Alireza, F.; Sudhanshu, S.; Joel, W.; Ager, I.; Cynthia, S. L.; Bharat, J.; *Nature Communications*, **2017**, 8, 15167.
19. John, J.; Mahadevan, V.P.; Thomas, A.R.; Joseph, R.P.J.; Muthunatesan, S.; Raghavendran, V.; and Prabhu, R.; IOP Conf. Ser: Mater. Sci. Engg., **2017**, *195*, 012007.
20. Balamurugan, M.; Alagumalai, K.; Chen,T. W. C. S. M.; liu, X.; and Selvaganapathy, M.; *Microchemica Act*, **2021**, 188, 19.
21. Kurre, R.; Bajpai, S.; Bajpai, P.; *Mat. Sci. Appln*, **2018**, 9, 92.
22. Lagashetty,**A.;** Mittin,V.; Patil, M.K.; Ganiger, S.K.; *Poly. Bull.*, **2020**, *78(10)*, 5905.
23. Isiaka, O. O.; Taiwo, F. O.; Adeolu, A. A.; *I. J. Poly. Sci.*, **2020,** 8834518, 1.
24. Aruna, S.T.; Alexander, S.M.; Current Opinion in Solid State and Materials Science, **2008**, *12*, 44.
25. Lagashetty, A.; Havanoor, V.; Basavaraj, S.; Balaji, S.D and Venkataraman, A.; *Sci. & Tech. Adv. Mater.*, **2008**, 8, 484.
26. Bedre, M. D.; Basavaraj, S.; Balaji, S. D.; Shivakumar, V.; Lagashetty, A.; Venkataraman, A.; *Poly. Comp.*, **2009**, 30, 1668.